Progress In Electromagnetics Research M, Vol. 73, 47–59, 2018

SAR Calculation & Temperature Response of Human Body Exposure to Electromagnetic Radiations at 28, 40 and 60 GHz mmWave Frequencies

Tooba Hamed* **and Moazam Maqsood**

Abstract—The fast development of millimeter wave (mmWave) wireless communications and the associated concerns of potential negative impact on human health instigates the study on effects of mmWave frequency on the human body after exposure to electromagnetic field in terms of specific absorption rate (SAR) and temperature rise in computer simulation technology (CST). SAR distributions due to radiating source antenna were investigated using the finite difference time domain (FDTD) method in single and layered human tissues by examining the 1 g SAR (gram mass averaging) and point SAR (without mass averaging) at mmWave frequencies of 28, 40 and 60 GHz. The bioheat equation was used to find the temperature elevation in tissues. The FDTD grid size used in the computation was 1.00, 0.75, and 0.50 mm at 28, 40 and 60 GHz, respectively. The results concluded that at the radiated power of 20 and 24 dBm, SAR levels (without mass averaging) in the tissues at 28 GHz were less than 40 and 60 GHz. It was found that the temperature increase in the three layer model was 2–3 times higher than that in the single layer model. However, the temperature elevation never exceeded 1°C in all the determined cases which was well below the threshold value for the generation of any adverse thermal effects in the tissues. Moreover, the effect of distance between the source and tissue model was investigated. It was found that the SAR decreased as the distance increased from the radiating source. The results presented here will assist researchers in examining and simulating the performance of upcoming mmWave wireless networks in terms of exposure to human tissues.

1. INTRODUCTION

Concern of public health hazards is growing due to fast development and implementation of millimeter wave (mmWave) wireless communications. Recent research on mmWave is focused mainly on the 28, 40, 60 and 73 GHz bands. Therefore, there is a dire need to study the absorption of electromagnetic energy in human tissues due to the exposure to mmWave radiations. Safety guidelines standards are set by many countries to protect human bodies from exposure to radiations. Absorption tool which is widely used to determine the health hazards in the human body due to electromagnetic field (EMF) exposure is specific absorption rate (SAR). It is used to measure amount of power absorbed in the human mass [1].

If the power absorbed in the tissues after exposure to radiations is high, then it causes tissue heating. Another safety standard to check heating in the biological tissues is to measure temperature rise in human tissues [1, 2].

In present studies both SAR and temperature will be determined in the human tissues so that precautionary measures could be suggested to the end users of new technology in the form of wireless appliances.

Received 11 June 2018, Accepted 26 July 2018, Scheduled 6 September 2018

* Corresponding author: Tooba Hamed (toobahamed@yahoo.com).
The authors are with the Department of Electrical Engineering, Institute of Space Technology, Islamabad, Pakistan.

SAR is a function of many factors [20]. These factors affect the absorption of RF Field. SAR varies with features of the wave, features of the body and features of environment. About the features of the wave, the extent of SAR variation depends on the features of the signal, such as frequency [20] and polarization [21]. The present work addresses the dependence on the frequency. About the dependence with the body, the SAR value depends on the type of tissue (e.g., geometry [22]; size, age and dielectric properties [20] and tissue orientation/exact location [22] (e.g., the posture of the body; frontal or back incidence). This research addresses the dependence on the type of tissue. SAR also depends on the exposure conditions, e.g., environmental exposure (indoor and outdoor) and effects of other objects in the field near the exposed body [20]). The human exposure is greater in indoor environments than in outdoor environments, due to multipath rays, and mmWave communications is generally used for the indoor environments [3].

The mmWave band is a part of radio frequency spectrum that exhibits frequencies between 30 and 300 GHz with a small wavelength between 10 and 1 mm. The continuous increase in wireless communication traffic has resulted into increase in demand of high communication frequencies [3].

The reason of high appealing of mmWave frequencies for future mobile communication networks is the supply in larger amounts on contiguous bandwidth and multi-Gbps date rates in the mmWave band [4]. Advantageous use of high frequency transmission systems is that the size of antenna becomes smaller. This allows easier handling and higher number of antennas can be used to increase overall performance.

The mmWave communications experience huge propagation loss due to the high carrier frequency. Moreover, communications range is limited by rain attenuation, molecular and atmospheric absorption. Attenuation at large distances is more significant as listed in Table 1. However, trend of small cell access is useful, and the obstacles such as rain and atmospheric absorption have no considerable path loss for cell sizes on the order of 200 m. It is why mmWave communications is mainly used for the indoor environments [3].

Table 1. Performance characteristics of millimeter wave communications as function of distance.

Frequency	Rain Attenuation at 25 mm/h		Oxygen Absorption	
Band (GHz)	200 m	1000 m	200 m	1000 m
28	0.9 dB	4.5 dB	0.04 dB	0.2 dB
40	1.34 dB	6.7 dB	0.03 dB	0.18 dB
60	2 dB	10 dB	3.2 dB	16 dB

Current research in this paper is focused on 28, 40 and 60 GHz bands. Frequencies 28 and 40 GHz emerge as a strong candidate for future 5G due to following reasons. First, these bands have much lower absorption rates of oxygen than other high mmWave frequencies, thus making more viability of long distance communications. Secondly, multipath environment is favorable for these frequencies to function well and can be used further for non-line-of-sight communications [3]. 40 GHz has also been listed by International Telecommunication Union (ITU) as internationally feasible frequency for 5G standards [4].

Research on 60 GHz is also rising along with other emerging mmWave frequencies. Per Shannon, more bandwidth is equivalent to more data throughput, and hence 60 GHz has a big advantage over other frequencies. 60 GHz band gives attractive benefits for many applications: high immunity to interference, license free operation and easy cost effective deployment. 60 GHz also offers the advantages of security in comparison to other wireless technologies [5]. However, there is high absorption in the spectrum of 60 GHz transmission, due to oxygen molecules (O_2). The peak value at 60 GHz could be as high as 16 dB/km. This absorption by oxygen reduces the 60 GHz signal strength. The longer it travels, the more the signal is reduced, thus limiting the distances and links coverage [5].

This paper is structured as follows. It starts with the introduction. Section 2 summarizes the antenna performance analysis and design details. Methodology is discussed in Section 3. Main description about SAR calculation and temperature elevation in the tissues are detailed in Sections 3.1 & 3.3. Its dielectric properties are given in Section 3.2. Complete results of both SAR and temperature response at three frequencies are presented in Section 4 along with the discussions. Finally, Section 5 concludes this paper.

2. ANTENNA PERFORMANCE ANALYSIS AND DESIGN DETAILS

Current trend of research on antennas is to make antennas smaller, principally in personal wireless devices (e.g., cell phones). A lot of effort is being undertaken on numerical modeling of antennas. By this way their properties can be predicted earlier to build and then tested.

Microstrip antennas are mostly considered suitable for modern day gadgets due to their low cost, low profile, simple fabrication and easy replication for large arrays [6]. Microstrip antennas work well at higher frequencies as well, keeping the overall size much smaller.

In this study, a microstrip patch antenna array at 28, 40 and 60 GHz is designed in CST MWS by following the layout as given in [7] to measure the exposure on the human tissues.

A four-element array of rectangular patch antenna is used, and feeding of array is realized using

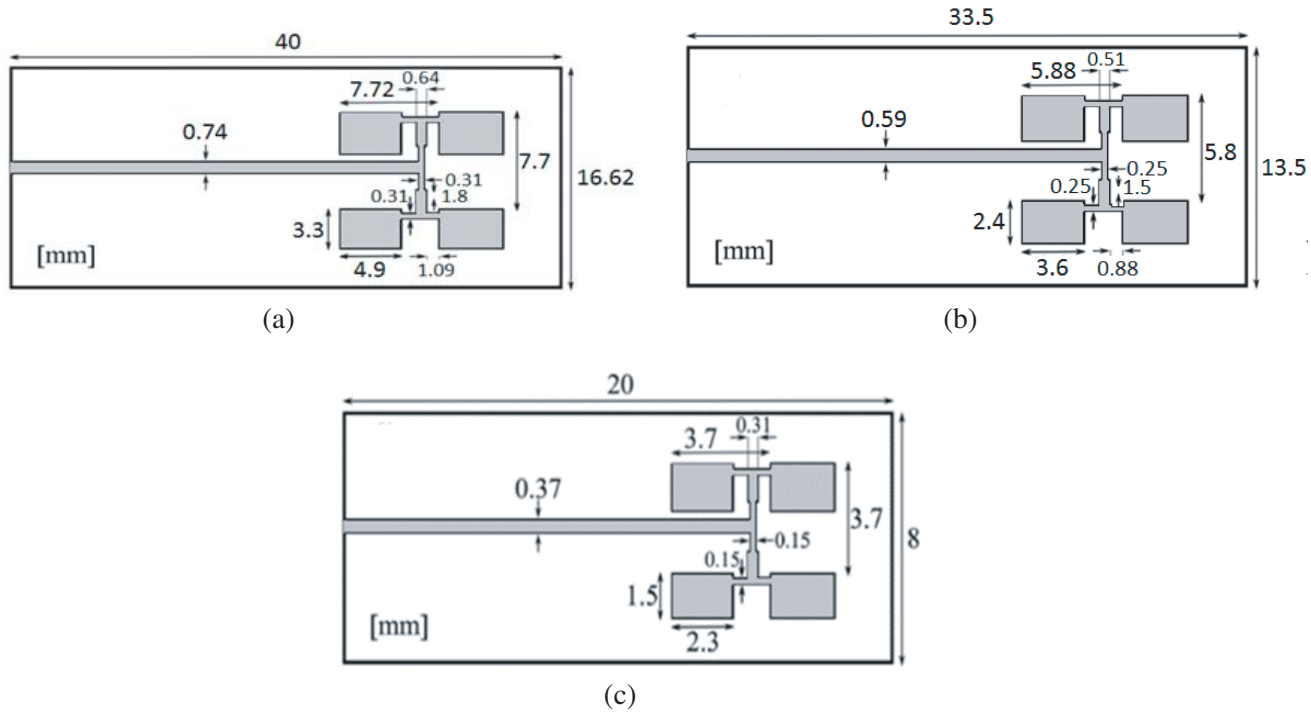

Figure 1. Schematic representation of 2×2-patch single layer antenna array at (a) 28 GHz, (b) 40 GHz, (c) 60 GHz [7].

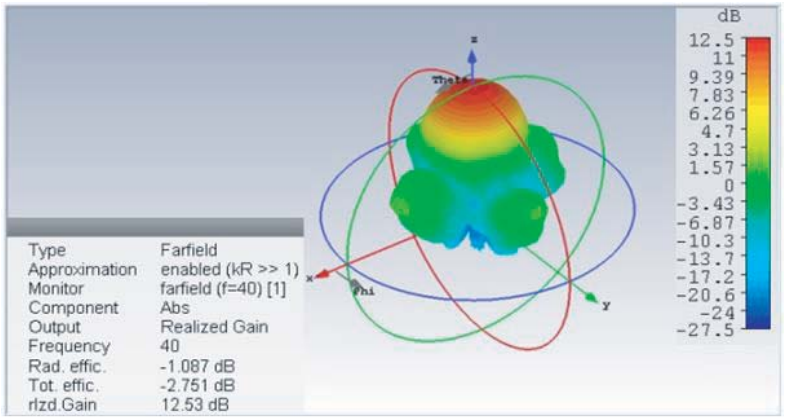

Figure 2. 2×2-patch antenna array 3D radiation pattern at 40 GHz.

coaxial feed. The patch array is designed with thickness of 0.0035 mm and placed over an RT/Duroid 5880 ($\varepsilon_r = 2.2$, $\tan\delta = 0.003$) substrate which is backed by very thin ground plane.

A 2×2 antenna array with inter-element spacing of (2.82, 4.4 mm at 28 GHz), (2.28 and 3.40 mm at 40 GHz) and (1.4, 2.2 mm at 60 GHz) is selected to accomplish a good tradeoff between high gain and low side lobes. The layout is represented in Fig. 1. The simulated gain values at designed frequencies are 11.23, 12.53, and 12.93 dB, respectively. The simulated gain at 40 GHz is shown in Fig. 2.

3. METHODOLOGY ON SAR CALCULATION AND TEMPERATURE RESPONSE

A unit of radiation absorption measurement, the Specific Absorption Rate, or SAR is an exposure standard for wireless devices to evaluate the hazards due to radio frequency wave. It is a measure of energy absorbed by the human tissue during exposure to a radio frequency (RF) electromagnetic per unit mass [2]. Exposure of the human body to a radio frequency field results in SAR which is proportional to the squared electric field strength value induced in the body [8].

SAR values are averaged either over whole body or a small portion of the sample (01 g or 10 g of tissues) [9]. The higher the SAR value is, the more the absorbed radiations are in the tissues and thus the more severe effects on human body. Guidelines are based on SAR thresholds where adverse health effects may occur [9].

3.1. SAR Calculation

SAR is the measure of the energy absorbed by mass placed in a volume with the mass density (p) of the tissue.

$$\mathrm{SAR}_i = P_i/\rho_i = \sigma_\iota |E|^2/2\rho_i \tag{1}$$

where, units of SAR are watts per kilogram (W/kg). P is the power loss density (watts per meter cube), ρ the density of human tissues (kilogram per meter cube), E the electric field strength (volts per meter), σ the conductivity (Siemens per meter) [10], and i the ith tissue.

To get information on the electromagnetic field distribution inside the tissue structure, it is required to define power loss density monitor. Power loss density and SAR monitor basically records the losses inside the calculation domain in the form of electric and magnetic losses and uses these losses as a source to compute SAR distribution in the tissues model.

At low radiated power levels, comparatively high field strengths would be estimated near the antenna when the antenna is close to the human model. The field distributions on the human tissues, when antenna is very close to human tissue, are usually measured in the near-field region of the antenna [11].

SAR calculation in terms of averaging scheme is also important to understand. There exist two methods to perform SAR calculations: one is point SAR, and other is averaging SAR (mass or volume). Point SAR is the value without mass averaging and defined the maximum SAR of all the grid cells, and point SAR for each grid cell is calculated by absorbed power in each grid divided by grid mass. In averaged SAR values, a cube with defined mass, e.g., 1 g or 10 g, is used for each point, and power loss density is integrated on this cube. At the end power loss in integral form is divided by the cube's mass.

Restriction limits of SAR for the general public are given in Table 2 [10, 12].

Table 2. SAR exposure limit guideline [12].

Standard	SAR Limit [W/kg]	Averaging mass for SAR
ICNIRP	2.0 ($f < 10$ GHz)	10 g of tissues
FCC/ANSI	1.6 ($f < 6$ GHz)	1 g of tissues

It is important to note that the ICNIRP guideline for SAR at frequency above 10 GHz and FCC guideline for SAR at frequency above 6 GHz are not provided yet. Because at mmWaves, near-field exposure has had a limited realistic concern so far, these guidelines even do not provide any dosimetric quantity or recommendations to be used for near-field exposure at mmWaves [7, 13].

Power density is used to measure the exposure above 6 GHz according to FCC guideline [8]. However, current recommendations by the FCC and ICNIRP organizations only deal with far-field exposures at distance equal to 5 cm or more than from the source. Evaluations based on the power density explain only the power travelling toward the tissue and do not explain the power absorption and field distribution in the tissues. So, power density is not considered useful to measure exposure in the near field at mmWaves [13], and SAR and temperature elevation techniques are used to study exposure at mmWaves frequencies.

3.2. Dielectric Properties of Human Tissues

Biological tissues constitute the layers of skin, fat, muscle and bone. Fig. 3 depicts a schematic geometry of structure of the tissue. Skin is an extremely complex tissue due to its inhomogeneous structure, leading to inhomogeneous dielectric properties. In general, skin has following layers: epidermis and dermis, and its thickness varies from 0.05 mm to 1 mm. The underside layers are fat and muscles with thicknesses of 3 mm and 20 mm [14].

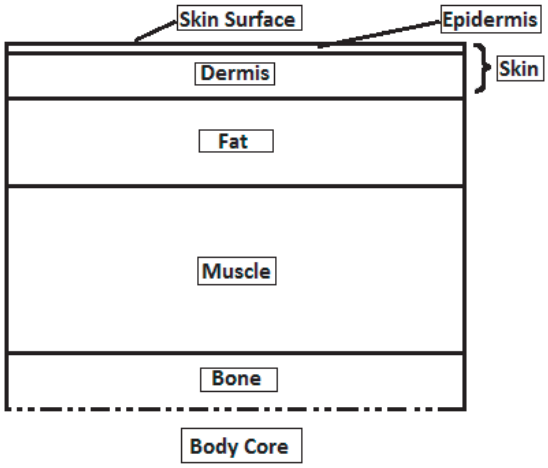

Figure 3. Schematic geometry of the structure of tissues.

The dielectric properties of the tissues (conductivity, relative permittivity) are important to determine while studying the propagation characteristic of mmWave. These properties control the reflection, propagation and attenuation of electromagnetic fields in the body and strongly depend on the tissue type and the frequency of interest.

Large differences occur in electric properties of bio-materials. Fluid content of the bio-material is usually used to determine these differences. For instance, electric current is conducted relatively well in blood and brain. Skin, bone and fat are comparatively poor conductors. Muscle bodies come under intermediate in their conductivities.

A detailed review regarding electrical properties of different tissues over wider frequency range is found in research articles by Gabriel et al. [15] to parameterize tissue dielectric properties. Such parameterization enables the calculation of reasonable estimate of the conductivity and permittivity at any frequency for different types of tissues [14].

Figures 4 and 5 show the relative permittivity and conductivity of skin versus frequency [13]. The permittivity and frequency have inverse relationship; therefore, permittivity of skin decreases as the frequency increases, whereas the conductivity of the skin increases (as the water content in the tissue increases) with the increase of frequency which show a direct relationship [19].

To quantify energy absorption and temperature rise in the human tissues due to electromagnetic field radiation, our research approach uses a tissue model. Tissue model shows dielectric characteristics in the same way as that of a human body, thereby, named a human equivalent model. To quantify energy absorption inside the human body, simulation is an effective technique.

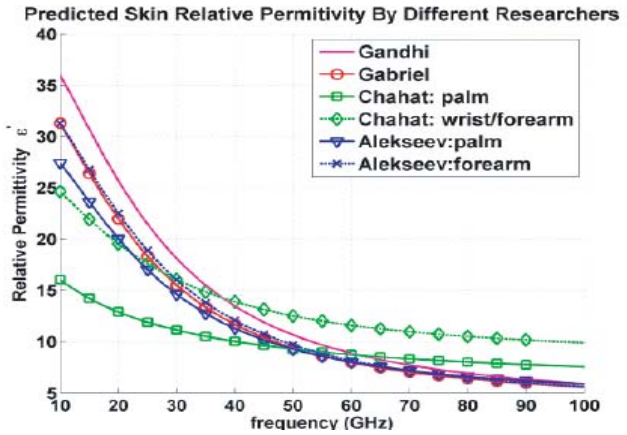

Figure 4. Permittivity of skin versus frequency [13].

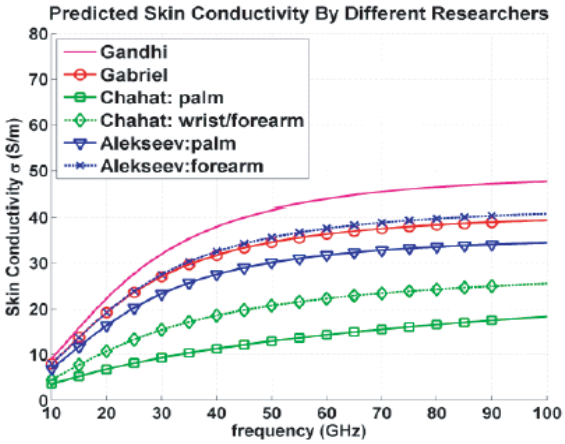

Figure 5. Conductivity of skin versus frequency [13].

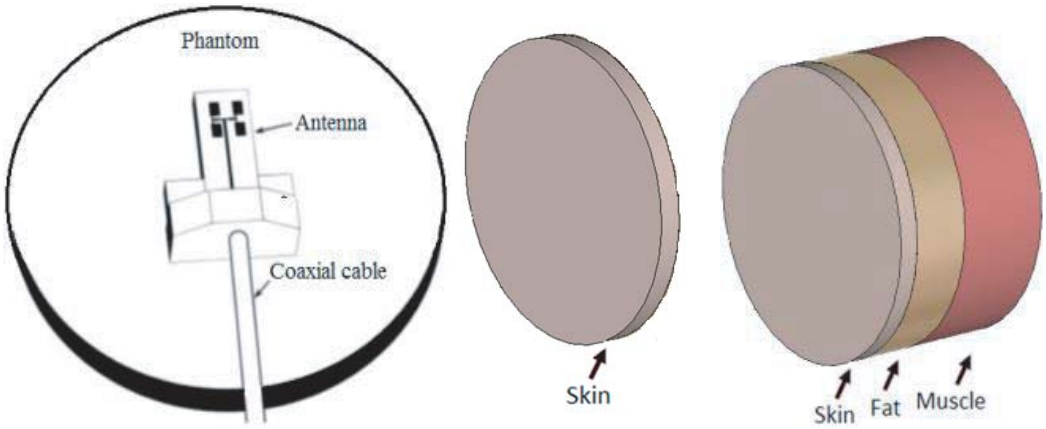

Figure 6. Shematic representation of tissues, (a) cylindrical equivalent phantom with antenna mounted on it [7], (b) single layer model, (c) three layer model.

In this study, tissue model in a cylindrical phantom form is used with a diameter of 70 mm and thickness of 7 mm. 5.5 mm spacing is set between antenna and tissue models. The FDTD grid sizes used in the computation are 1.00, 0.75, and 0.50 mm at 28, 40 and 60 GHz, respectively. Fig. 6(a) shows the schematic representation of antenna placed on a cylindrical equivalent phantom, and single and three layer phantoms can be seen in Figs. 6(b) and (c).

Table 3 indicates the electrical properties of different tissues used in tissue models at 28, 40 and 60 GHz [15].

Table 3. Dielectric properties of human tissues.

Tissue	Mass Density	Relative Permittivity [ε_r]			Conductivity [S/m]		
	[kg/m^3]	28 GHz	40 GHz	60 GHz	28 GHz	40 GHz	60 GHz
Skin	1109	16.55	11.69	7.98	25.82	31.78	36.38
Muscle	1090	24.43	18.24	12.86	33.6	43.13	52.80
Fat	911	6.09	5.21	4.40	5.04	6.58	8.39

3.3. Temperature Elevation in the Tissues

During the previous decade, an exciting interest has been in phenomena of bio-heat transfer, emphasizing particularly on applications of diagnostic and new technology effects on human tissues.

Temperature assessment in the human bodies is necessary as electromagnetic exposure can cause severe health effects by inducing excessive temperature to the exposed tissue and thus damaging the human tissues.

Temperature distributions in tissue during radio frequency wave's exposure can be measured by solving the equation of bio-heat transfer [16]. Firstly the SAR distribution by the external source is calculated, then geometrical parameters and thermal properties are added in model. The information obtained with suitable boundary conditions is used to calculate tissue temperature distribution.

In bio-heat equation, SAR is related as follows [16]:

$$c\rho\partial T/\partial t = \nabla \cdot (k\nabla T) + \rho(\text{SAR}) + A - B(T - T_b) \tag{2}$$

where $B = c_b W_b$; c_b equals tissue specific heat; W_b equals blood perfusion coefficient; ρ equals tissue density; k equals tissue thermal conductivity; T equals local temperature of tissue; A represents basal metabolic heat rate; T_b equals blood temperature; $\nabla \cdot (k\nabla T)$ represents simple heat equation in differential form; ρ(SAR) represents the influence of electromagnetic energy absorbed in the human tissues.

Blood temperature T_b is basically independent of the SAR value as electromagnetic radiations heat does not change the basal body temperature. The blood temperature (T_b) and atmospheric temperature (T) are set to 37°C and 20°C, respectively.

Thermal boundaries are set as adiabatic boundary (in which temperature distribution is not constant and no heat flow occurs) parallel to the waveguide port, and isothermal boundary is set (through which heat flow occurs but the temperature is considered as constant) in remaining directions. Thermal parameters of this study are put in Table 4 [13].

Table 4. Thermal parameters of human tissues.

Tissue Properties	Unit	Skin	Fat	Muscle
Density (Rho)	Kg/m^3	1109	911	1090
Heat capacity	kJ/K/kg	3.391	2.348	3.421
Thermal conductivity	W/K/m	0.37	0.21	0.49
Metabolic rate	W/m^3	1620	300	480
Tissue Thickness	mm	1	3	4

IEEE and ICNIRP set electromagnetic safety standards after providing threshold limits for the temperature rise in the human tissues due to electromagnetic energy exposure in [17].

4. RESULTS AND DISCUSSION

A SAR calculation and temperature elevation measurement system are implemented to investigate power absorption and temperature increase in the tissues of human body using 20 and 24 dBm radiated power at 28, 40 and 60 GHz.

Results in single layer model with 20 and 24 dBm radiated power are shown in Figs. 7(a) and (b), Figs. 8(a) and (b), Figs. 9(a) and (b), Figs. 10(a) and (b), Figs. 11(a) and (b) and Figs. 12(a) and (b), respectively. SAR values ae high on the tissues model near the antennas and low at the surroundings tissues.

In Table 5, SAR results at radiated power of 20 dBm are summarized at all the frequencies.

The maximum 1 g averaged SAR of 0.885 W/kg is found at 60 GHz (with antenna/tissue spacing of 5.5 mm), and this value is larger than 1 g averaged SAR values at 28 and 40 GHz. Result concludes that the maximum power absorption in tissues is at 60 GHz compared to 28 and 40 GHz. Moreover, we get a dip in SAR value at 40 GHz. So, we conclude that minimum absorption in tissues is at 40 GHz with averaging method.

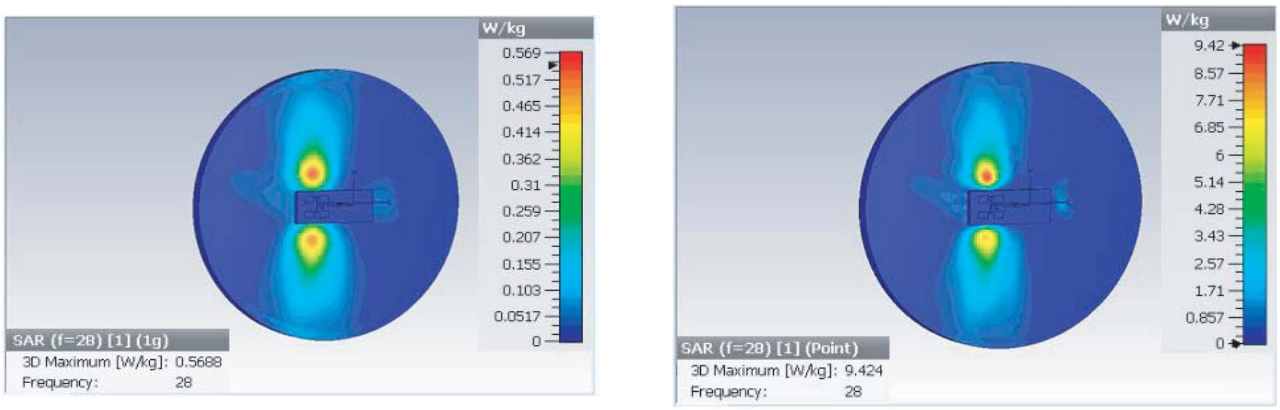

(a) (b)

Figure 7. SAR [W/kg] in single layer model at 28 GHz with 20 dBm simulated power, (a) 1 g SAR, (b) point SAR.

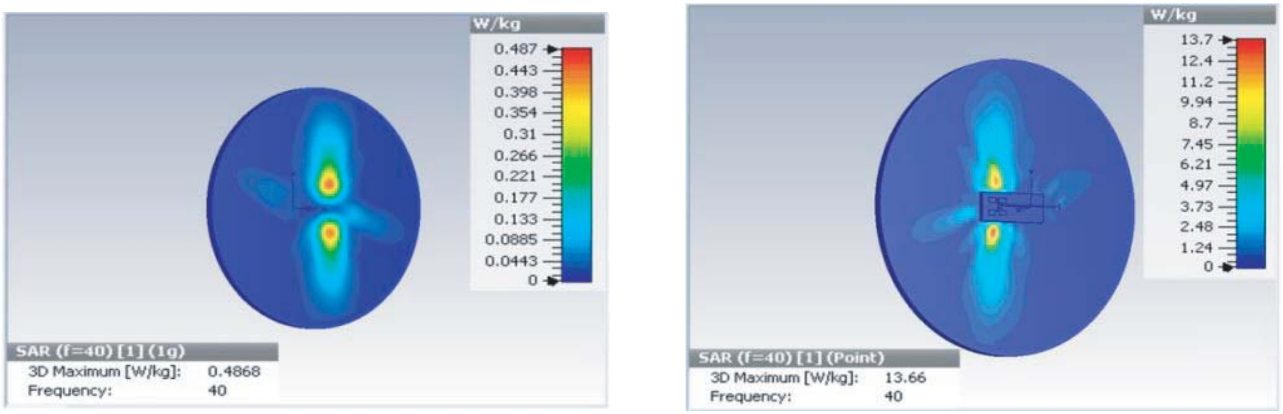

(a) (b)

Figure 8. SAR [W/kg] in single layer model at 40 GHz with 20 dBm simulated power, (a) 1 g SAR, (b) point SAR.

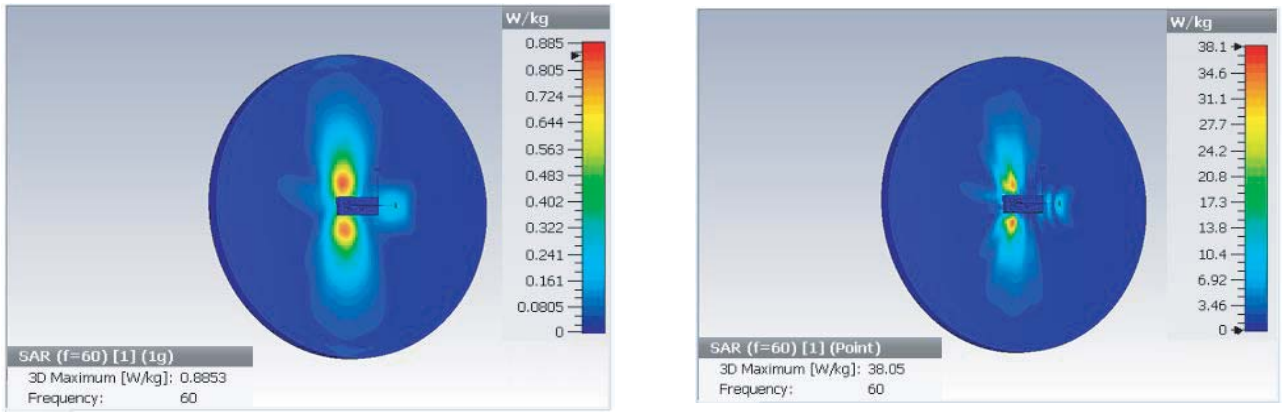

(a) (b)

Figure 9. SAR [W/kg] in single layer model at 60 GHz with 20 dBm simulated power, (a) 1 g SAR, (b) point SAR.

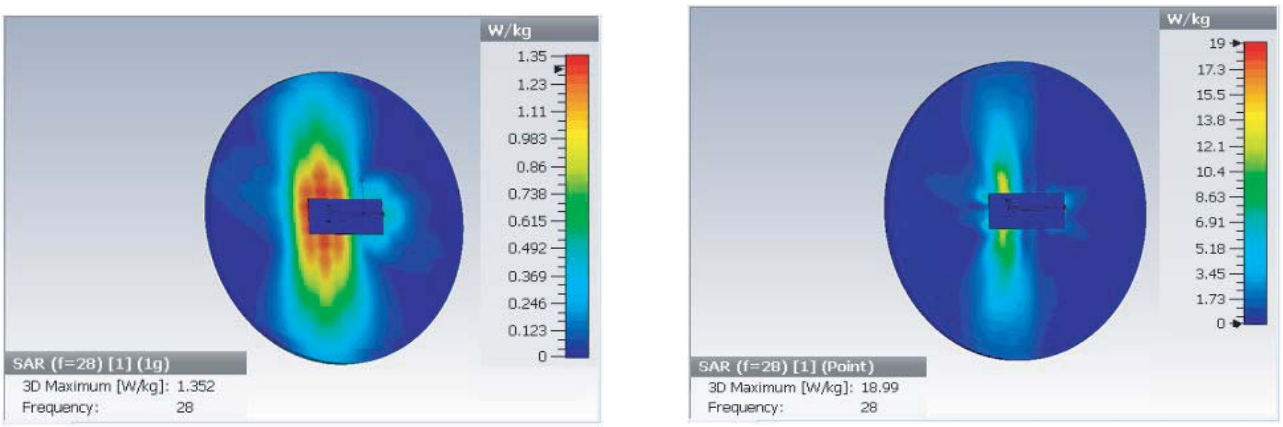

(a) (b)

Figure 10. SAR [W/kg]in single layer model at 28 GHz with 24 dBm simulated power, (a) 1 g SAR, (b) point SAR.

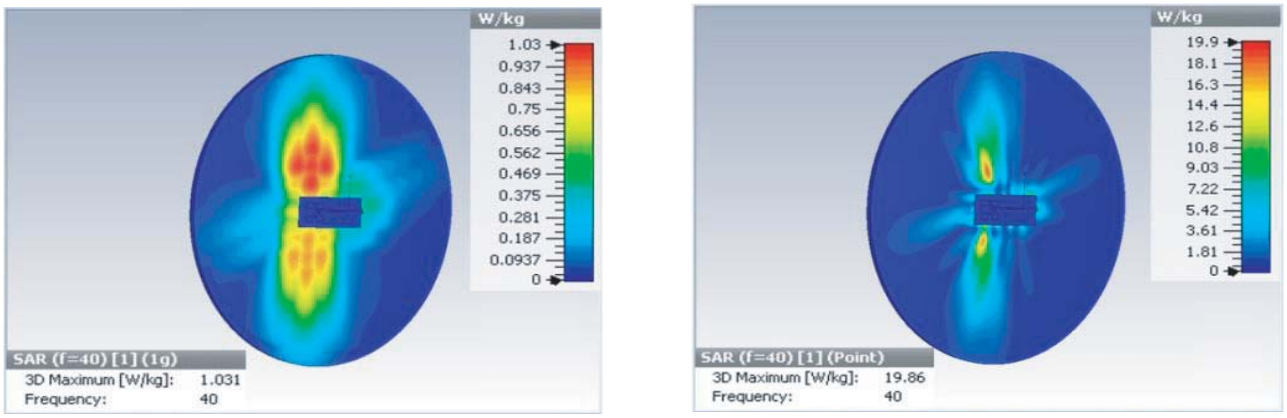

(a) (b)

Figure 11. SAR [W/Kg] in single layer model at 40 GHz with 24 dBm simulated power, (a) 1 g SAR, (b) point SAR.

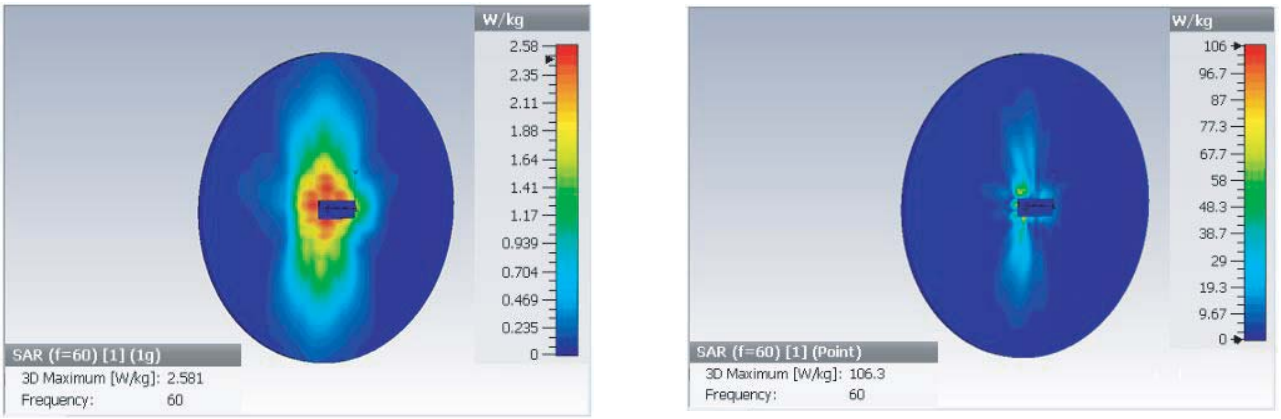

(a) (b)

Figure 12. SAR [W/kg] in single layer model at 60 GHz with 24 dBm simulated power, (a) 1 g SAR, (b) point SAR.

Table 5. SAR at radiated power of 20 dBm.

Frequency [GHz]	28	40	60
Maximum SAR (1 g) [W/Kg]	0.568	0.486	0.885
Maximum Point SAR [W/Kg]	9.423	13.66	38.05
Total SAR [W/Kg]	0.049	0.035	0.054

Table 6. SAR at radiated power of 24 dBm.

Frequency [GHz]	28	40	60
Maximum SAR (1 g) [W/Kg]	1.352	1.030	2.581
Maximum Point SAR [W/Kg]	18.99	19.861	106.31
Total SAR [W/Kg]	0.183	0.145	0.216

Point SAR value (calculated without mass averaging) at 60 GHz is 38.05 W/kg, which is higher than the point SAR values at 28 and 40 GHz. Point SAR results show that SAR value increases with the increase of frequency. Our results agree with those presented in findings [12].

In Table 6, we conclude that by increasing the radiating power of antenna from 20 dBm to 24 dBm, SAR values are increased for all three frequencies. In both SAR calculation methods, results received at 60 GHz are higher than those at 28 and 40 GHz. We also examine that averaged SAR results are less than point SAR results at both radiated powers.

Now, SAR averaged over 1 g of mass and point SAR is measured by considering three tissues, skin, fat and muscles, at 20 dBm radiated power.

SAR values of 0.976 and 37.1 W/kg show the areas of maximum power absorption in the tissues at 60 GHz in Figs. 15(a) and (b). The total SAR is 0.127 W/Kg. Results in Figs. 13, 14 and 15 conclude that the three layer tissues model shows SAR values bit higher than single layer tissues model.

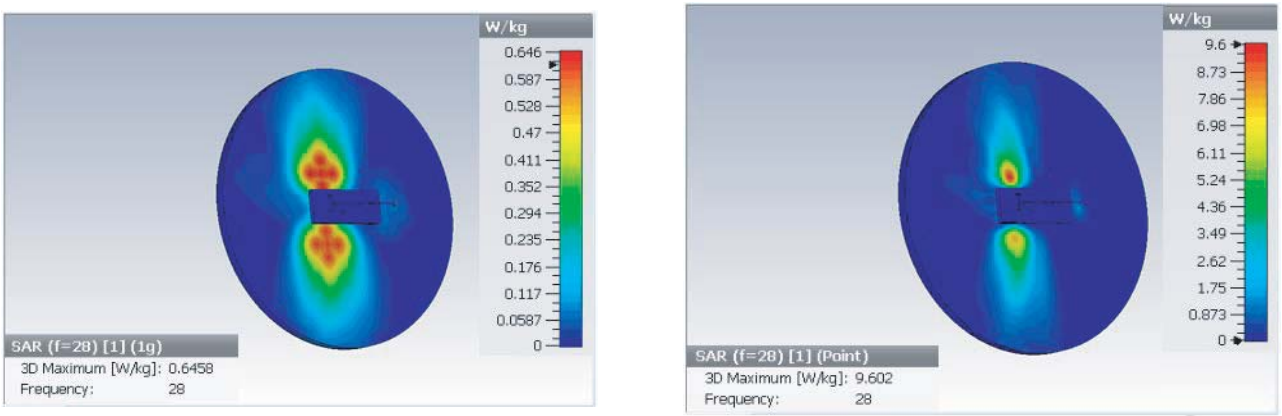

(a) (b)

Figure 13. SAR [W/kg] at 28 GHz in three layer model with 20 dBm simulated power, (a) 1 g SAR, (b) point SAR.

Temperature response system is implemented to investigate temperature increase in human tissues. However, temperature rise in human tissues is caused by many factors, such as external radiation source, bioheat properties of tissues (metabolic heat and blood flow) and thermal properties of tissues (density and thermal conductivity) [16].

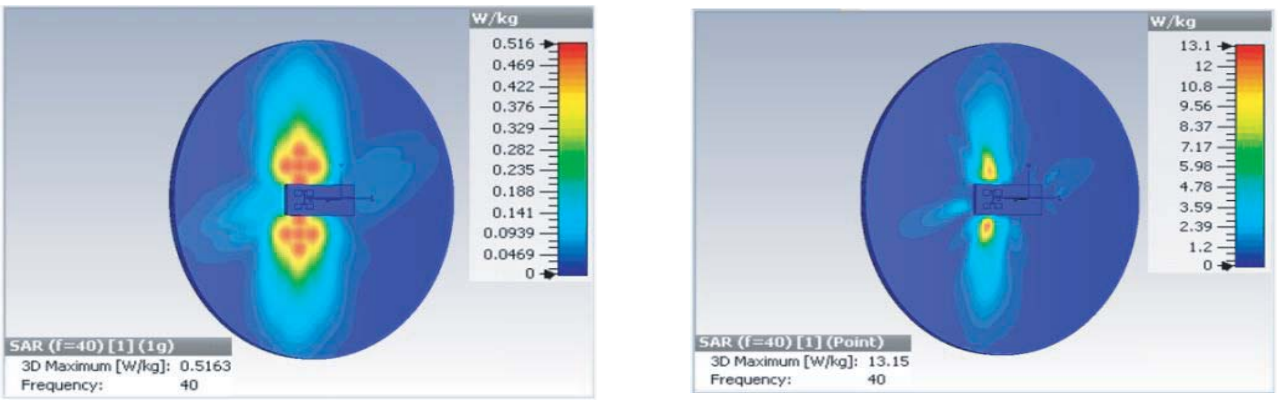

(a) (b)

Figure 14. SAR [W/Kg] at 40 GHz in three layer model with 20 dBm simulated power, (a) 1 g SAR, (b) point SAR.

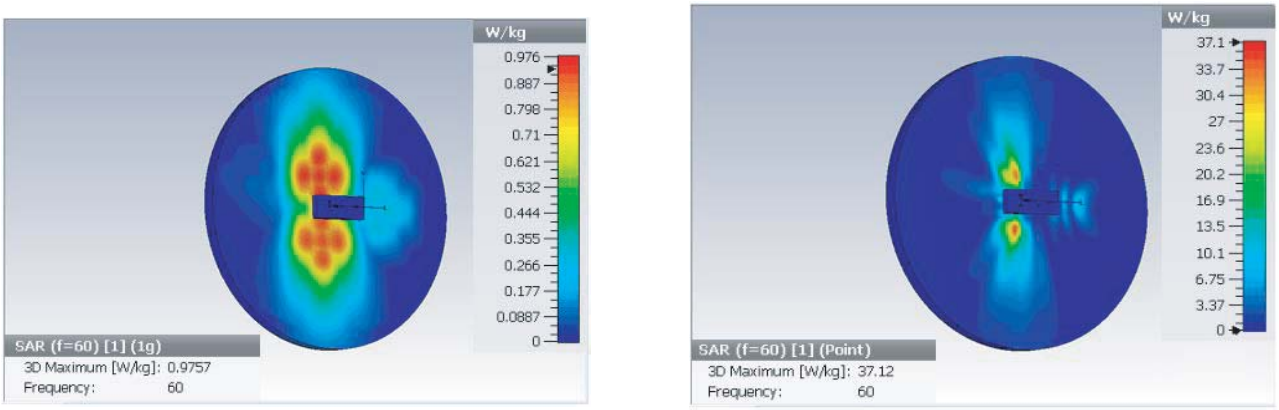

(a) (b)

Figure 15. SAR [W/kg] at 60 GHz in three layer model with 20 dBm simulated power, (a) 1 g SAR, (b) point SAR.

In this study, higher temperature increase of 0.21°C is found at 60 GHz in single tissue model (Table 7). These results agree with those explained in finding in [7] where temperature rise of 0.20°C was recorded at 60 GHz. The maximum temperature rise of 0.59°C is found at 60 GHz in three layer model, but this value is below the acceptable temperature limit (1°C) according to safety limit guidelines by IEEE on mmWave radiations [17].

Results in Table 7 conclude that the temperature increase in the three layer model is 2–3 times higher than in the single layer model. Present results show conformity with the literature [18].

SAR and temperature values are within limits, but due to the emergence of smart phones, running of background apps for continuous transferring of data combined with constant close proximity with human body, long term damages can be caused.

Table 7. Temperature elevation at radiated power of 20 dBm.

Frequency [GHz]	28	40	60
Single Layer Tissues	0.18°C	0.11°C	0.21°C
Three Layer Tissues	0.5°C	0.3°C	0.59°C

Table 8. SAR as function of distance at radiated power of 24 dBm.

Distance [mm]	0.5	3	5
Maximum SAR (1 g) [W/Kg]	5.602	1.837	1.352
Maximum Point SAR [W/Kg]	91.7	23.868	18.99
Total SAR [W/Kg]	0.407	0.203	0.183

To study the effect of spacing between radiating source and tissue model, simulation results are computed at distances of 0.5, 3 and 5.5 mm between source and tissues (Table 8). The depicted results are given at 28 GHz. Maximum 1 g SAR of 5.60 W/kg is found in the tissues, when the antenna/source spacing was 0.5 mm. It is concluded that the SAR induced in the tissues decreases with the distance from the radiating source. Our results are in close agreement with those presented in findings in [2, 7].

5. CONCLUSION

Effects of radiation on human tissue due to mmWave exposure at 28, 40 and 60 GHz have been studied. Human tissue sample is modeled, exposed to radiating source, and the exposure effects are quantified in terms of SAR and temperature elevation. SAR distributions in the human tissues in all the situations at 60 GHz have been found higher than 28 and 40 GHz. In all formulated models, temperature elevation in the human tissues have never exceeded 0.59°C which is below the temperature threshold of 1°C.

REFERENCES

1. Zhadobov, M., N. Chahat, R. Sauleau, C. L. Quement, and Y. L. Drean, "Millimeter-wave interactions with the human body: State of knowledge and recent advances," *International Journal of Microwave and Wireless Technologies*, 2011.
2. Sabbah, A. I., N. I. Dib, and M. A. Al-Nimr, "Evaluation of specific absorption rate and temperature elevation in a multi-layered human head model exposed to radio frequency radiation using the finite difference time domain method," *IET Microwave Antennas Propag.*, Vol. 5, 1073–1080, 2011.
3. Niu, Y., Y. Li, D. Jin, L. Su, and A. V. Vasilakos, "A survey of millimeter wave (mmWave) communications for 5G: Opportunities and challenges," *Wireless Networks*, Vol. 21, 2657–2676, 2015.
4. Millimeter Wave: "The battle of the bands," National Instrument, [online], available: http://www.ni.com/white-paper/53096/en/, 2016.
5. 60 GHz Wireless Technology Overview, http://www.mmwaves.com/products.cfm/product/20-194-0.htm, accessed Nov. 20, 2016.
6. Rashid, M. and S. Hossain, "Antenna solution for millimeter wave mobile communication (MWMC): 5G," *International Journal of Scientific Research Engineering & Technology (IJSRET)*, Vol. 3, 1157–1161, 2014.
7. Chahat, N., M. Zhadobov, L. Le Coq, S. Alekseev, and R. Sauleau, "Characterization of the Interactions between a 60-GHz antenna and the human body in an off-body scenario," *IEEE Transactions on Antennas and Propagation*, Vol. 60, 5958–5965, 2012.
8. Robert, F. C., L. U. Jerry, Jr., and L. M. David, "Evaluating compliance with FCC guidelines for human exposure to radiofrequency electromagnetic fields," OET Bulletin 65, Federal Communications Commission, 1997.
9. Wittig, T., "SAR overview," www.cst.com, accessed Nov. 25, 2016.
10. Aly, A. A. and M. Piket May, "FDTD computation for SAR induced in human head due to exposure to EMF from mobile phone," *Advanced Computing an International Journal*, Vol. 5, 2014.
11. David, M. and W. Kwok, "Additional information for evaluating compliance of mobile and portable devices with FCC limits for human exposure to radiofrequency emission," OET Bulletin 65, Federal Communications Commission, 2001.

12. Gustrau, F. and A. Bahr, "W-band investigation of material parameters, SAR distribution, and thermal response in human tissue," *IEEE Trans. on Microwave Theory Tech.*, Vol. 50, 2393–2400, 2002.
13. Wu, T., T. S. Rappaport, and C. M. Collins, "The human body and millimeter wave wireless communication systems: Interactions and implications," *IEEEInternational Conference on Communications*, London, UK, 2015.
14. Miklavcic, D. and N. Pavselj, "Electric properties of tissues," *Wiley Encyclopedia of Biomedical Engineering*, 2006.
15. Gabriel, C., S. Gabriely, and E. Corthout, "The dielectric properties of biological tissues: I. Literature survey," *Phys. Med. Biol.*, Vol. 41, No. 11, 2231–2249, 1996.
16. Strydom, M. and T. Wittig, "Bioheat simulations with CST studio suite," [online], available: https://www.cst.com/Content/Events/UGM2009/6-2-4-Bioheat-simulations-with-CST-STUDIO-SUITE.pdf, 2009.
17. "IEEE Standard for Safety Levels with respect to Human Exposure to the Radio Frequency Electromagnetic Fields 3 kHz to 300 GHz," IEEE Std., C95.1, 2005.
18. Kanezaki, A., A. Hirata, S. Watanabe, and H. Shirai, "Parameter variation effects on temperature elevation in a steady-state, one-dimensional thermal model for millimeter-wave exposure of one- and three-layer human tissue," *Phys. Med. Biol.*, Vol. 55, No. 16, 4647–4659, 2010.
19. Wang, J. and Q. Wang, *Body Area Communications: Channel Modeling, Communication Systems, and EMC*, 1st Edition, John Wiley & Sons Singapore PTE Ltd, ISBN: 978-1-118-18848-4, 2013.
20. [ICNIRP1998] International Commission on Non-Ionizing Radiation Protection (ICNIRP), "Guidelines for limiting exposure to time-varying electric, magnetic and electromagnetic fields (up to 300 GHz)," *Health Phys.*, Vol. 74, No. 4, 494–522, 1998.
21. Miguel-Bilbao, S., V. Ramos, and J. Blas, "Comments on assessment of polarization dependence of body shadow effect on dosimetry measurements in the 2.4 GHz band," *Bio-electromagnetics*, Vol. 38, No. 4, 315–321, 2017.
22. Uusitupa, T., I. Laakso, S. Ilvonen, and K. Nikoskinen, "SAR variation study from 300 to 5000 MHz for 15 voxel models including different postures," *Phys. Med. Biol.*, Vol. 55, No. 4, 1157–1176, 2010.